RSC Advances




ROYAL SOCIETY OF CHEMISTRY

www.rsc.org/advances

RSC Advances

RSCPublishing

ARTICLE

# Effects of Alkyl or Alkoxy Side Chains on the Electrochromic Properties of Four Ambipolar Donor-Acceptor Type Polymers

Yanxia Liu, Min Wang, Jinsheng Zhao*, Chuansheng Cui and Jifeng Liu*

Cite this: DOI: 10.1039/x0xx00000x

Received ooth January 2012,
Accepted ooth January 2012

DOI: 10.1039/x0xx00000x

www.rsc.org/

Four donor-acceptor type π-conjugated polymers, poly[2,3-di(2-furyl)-5,8-bis(2-(4-butoxythiophene)) quinoxaline] (PFBOTQ), poly[2,3-di(5-methylfuran-2-yl)-5,8-bis(2-(4-butoxythiophene)) quinoxaline] (PMFBOTQ), poly[2,3-di(2-furyl)-5,8-bis(2-(4-butylthiophene)) quinoxaline] (PFBTQ) and poly[2,3-di(5-methylfuran-2-yl)-5,8-bis(2-(4-butylthiophene)) quinoxaline] (PMFBTQ) containing 2,3-di(2-furyl) quinoxaline or 2,3-di(5-methylfuran-2-yl) quinoxaline moiety in the backbone as the acceptor unit and different thiophene derivatives as donor units are synthesized electrochemically. The four polymers are characterized by cyclic voltammetry (CV), UV-Vis-NIR spectroscopy, scanning electron microscopy (SEM) and step profiler. Both PFBOTQ and PMFBOTQ with strong electron-donating butoxy group have lower oxidation potentials than that of PFBTQ and PMFBTQ, respectively. Electrochemical measurements and Spectroelectrochemistry analyses demonstrate that all four polymers exhibit both p- and n-type doping processes. Both PFBOTQ and PMFBOTQ exhibit a green color in the neutral state, while PFBTQ with two absorption bands at 349 nm and 541 nm is light purplish red color and PMFBTQ with one obvious absorption band at 349 nm as well as a shoulder peak located at around 500 nm show light brown-red color in the neutral state. Furthermore, as typical donor-acceptor polymers, all four polymers present robust stabilities, low optical band gaps, excellent optical contrasts in NIR region, satisfactory coloration efficiencies and fast switching times which make four polymers outstanding candidates for electrochromic applications.

## 1. Introduction

A great deal of attention has been focused on conductive polymers since the discovery[1] of conductivity polyacetylene upon doping and then the conductive polymers turned out to be key materials in a broad range of practical applications such as polymer light-emitting diodes,[2,3] photovoltaic devices,[4] sensors,[5] field effect transistors,[6,7] smart windows,[8] camouflage materials[9,10] and electrochromic devices.[11-14] Among the conductive polymers, electrochromic (EC) polymers have arisen public concern due to that the polymers can reversibly change color from the same material by altering its redox state. And then electrochromic conjugated polymers have received enormous attention due to the huge advantages of high optical contrasts, fast switching times, superior coloration efficiencies, fine-tuning of the band gaps by structure modification, the lower costs and processibilities compared to many inorganic oxides (tungsten, iridium and nickel oxides, etc) materials.[15-19]

However, the problem was that huge amounts of electrochromic polymers can be hardly used in practical electrochromic devices applications due to their relatively high band gaps. So most efforts in the electrochromic polymers were on the design and synthesis the macromolecule electrochromic conjugated polymers contained alternating electron rich (donor, D) and electron poor (acceptor, A) units[20] which can significantly decrease the band gaps related to the electrochemical and optical of the polymers due to resonances that enabled a stronger double band character between donor and acceptor units.[21] The donor-acceptor polymer systems with low band gaps can easily obtain the multiple color changes by altering its different applied potentials corresponding to different redox states (p-type or n-type doping) because of the interchain charge transfer.[22,23] Meanwhile, the optical band gaps and the redox potentials that controlled the coverage of the optical absorption were easily tuned by altering the donor-acceptor systems. Furthermore, it was well known that the three leg (green) of color space (red-green-blue, RGB) has remained elusive.[24] The problem was that the green polymeric electrochromics should have at least two absorption bands (blue and red) at their neutral state in visible region and should also deplete simultaneously during oxidation.[25] This problem came to the end due to the combination of donor-acceptor units by the work of Wudl and Sönmez et al..[26] Recently reported paper about naphthalenediimide bridged D-A polymers also revealed the excellent electrochromic properties of D-A polymers.[27] Therefore, D-A systems have drawn lots of attention by their superiorities on electrochromics. The aromatic compounds with electron-

withdrawing imine nitrogens (C=N) as acceptor units identified as the representative acceptor-type building blocks[28,29] and different thiophene derivatives as donor units have obtained greatly attentions so as to design and synthesize the alternating systems during the past years.[19,24] Recently, quinoxaline derivatives as this kind of organic acceptor units contained in donor-acceptor electrochromic conjugated polymers have arisen much attentions due to that quinoxaline-fused ring has the significantly advantages of a firm coplanar backbone and a highly extensive π-electron conjugated system with strong π-stacking[30] which was a must for polymeric electrochromic materials.

It should be noted that polymers of this system usually not only have low band gap but also can reveal n-doped character. As is well-known, only a fraction of the conjugated polymers can exhibit n-doped property due to the poor stability at the reduction potential leading to the n-doping state. The n-doped electrochromic conjugated polymers are expected to have a great contribution to organic electronics in the near future since it will be possible for the fabrication of bipolar transistors and polymeric analogue of silicon field effective transistors.[31] Thus, the electrochromic conjugated polymers with stable negatively doped states have drawn great attention in the electrochromism field.

Following this strategy, our group previously reported the synthesis of poly[2,3-di(5-methylfuran-2-yl)-5,8-bis(2-(3-methoxythiophene)) quinoxaline] (PMFMQ) and poly[2,3-di(5-methylfuran-2-yl)-5,8-bis(2-thienyl) quinoxaline] (PMFTQ) containing strong electron-accepting 2,3-di(5-methylfuran-2-yl) quinoxaline as acceptor unit. Both of them presented lower optical band gaps and significant n-type doping processes.[32] In this paper, considering the contribution of the steric interaction between repeat units within the polymer backbone, using more planar system can result in better orbital overlap, thereby lowering the band gap.[33] So, 2,3-di(2-furyl) quinoxaline moiety with stronger electron-accepting ability and coplanarity was used as the substitute of the previous acceptor unit. Besides, butoxythiophene and butylthiophene were used as the substitutes of the previous donor units in order to study the effect on the electrochromic properties made by the increase of the alkyl chain length of the substituent on thiophene moiety. As a result, four novel monomers including 2,3-di(2-furyl)-5,8-bis(2-(4-butoxythiophene)) quinoxaline (FBOTQ), 2,3-di(5-methylfuran-2-yl)-5,8-bis(2-(4-butoxythiophene)) quinoxaline (MFBOTQ), 2,3-di(2-furyl)-5,8-bis(2-(4-butylthiophene)) quinoxaline (FBTQ) and 2,3-di(5-methylfuran-2-yl)-5,8-bis(2-(4-butylthiophene)) quinoxaline (MFBTQ) were synthesized beforehand. Then the corresponding polymers (PFBOTQ, PMFBOTQ, PFBTQ and PMFBTQ) were electrochemically synthesized respectively. Herein, we wish to unveil our results concerning the design, synthesis, electrochemical and optical properties of the four novel D-A-D type compounds. It was noteworthy that the polymers with the different acceptor and different donor units presented significantly differences of the electrochemical and optical properties due to the effects of the different donor and acceptor units. In particular, PFBOTQ and PMFBOTQ exhibited a green color in the neutral state and a highly transmissive oxidized state, which was of high value in fabricating smart electrochromics.

All four polymers showed low oxidation potentials, robust stabilities, high optical contrasts, satisfactory coloration efficiencies (CE) and extremely fast response times although their onset oxidation potentials and optical contrasts had slightly lower than that of the reported ones. What's more, generation of redox waves in CV curves at negative potentials and variation of the spectral absorption curves upon reduction proved that all four polymers had stable n-doping properties. These characteristics make the polymers of important application prospects in the field of smart electrochromism.

## 2. Experimental

### 2.1 Materials

3-butoxythiophene (99%), 3-butylthiophene (99%), furfural, 5-methylfurfural, copper sulfate pentahydrate ($CuSO_4 \cdot 5H_2O$), pyridine (98%), vitamin B1, sodium, sodium hydroxide (NaOH), 4,7-dibromo-2,1,3-benzothiadiazole (98%), P-toluene sulfonic acid (PTSA, 98%), sodium borohydride ($NaBH_4$, 98%), bis(triphenylphosphine) dichloropalladium ($Pd(PPh_3)_2Cl_2$), anhydrous ethyl alcohol (EtOH, 99.9%), acetone, n-butyllithium (2.5 M) and chlorotributyltin (97%) were all purchased from Aladdin Chemical Co., Ltd., China and used as received. Commercial high-performance liquid chromatography grade acetonitrile (ACN, Tedia Company, INC., USA) and dichloromethane (DCM, Sinopharm Chemical Reagent Co., Ltd., China) were used as received without further purification. Tetrabutylammonium hexafluorophosphate ($TBAPF_6$, Alfa Aesar, 98%) was dried in vacuum at 60 ºC for 24 hours before use. Tetrahydrofuran (THF, Tianjin windship chemistry Technological Co., Ltd., China) was distilled over Na in the presence of benzophenone prior to use. Indium-tin-oxide-coated (ITO) glass (sheet resistance: < 10 Ω $\square^{-1}$, purchased from Shenzhen CSG Display Technologies, China) was washed with ethanol, acetone and deionized water successively under ultrasonic, after that dried by $N_2$ flow.

### 2.2 Instrumentation

$^1$H NMR and $^{13}$C NMR spectra of the monomers were recorded on a Varian AMX 400 spectrometer in $CDCl_3$ at 400 MHz and chemical shifts (δ) were given relative to tetramethylsilane as the internal standard. The electrochemical behaviors were investigated by cyclic voltammetry (CV). And electrochemical syntheses and experiments were performed in a one-compartment cell with a CHI 760 C Electrochemical Analyzer under the control of a computer, employing a platinum wire with a diameter of 0.5 mm as working electrode, a platinum ring as counter electrode, and a Ag wire (0.02 V vs. SCE) as pseudo reference electrode. Scanning electron microscopy (SEM) measurements were taken by using a Hitachi SU-70 thermionic field emission SEM. The thickness and surface roughness of polymer films were carried on KLA-Tencor D-100 step profiler. UV-Vis-NIR spectra were recorded on a Varian Cary 5000 spectrophotometer connected to a computer. A three-electrode cell assembly was used where the working electrode was an ITO glass, the counter electrode was a stainless steel wire, and an Ag wire (0.02 V vs. SCE) was used as pseudo reference electrode. The polymer films for spectroelectrochemistry were prepared by potentiostatically deposition on ITO electrode (the active area: 0.9 cm ×3.0 cm). The thickness of the polymer films grown potentiotatically on ITO was controlled by the total charge passed through the cell. Digital photographs of the polymer films were taken by a Canon Power Shot A3000 IS digital camera.

### 2.3 Synthesis

#### 2.3.1 2,3-Bis(2-furyl)-5,8-dibromoquinoxaline (6) and 2,3-bis(5-methylfuran-2-yl)-5,8-dibromoquinoxaline (10)

5.75 g (19.56 mM) of 4,7-Dibromo-2,1,3-benzothiadiazole and 250



 

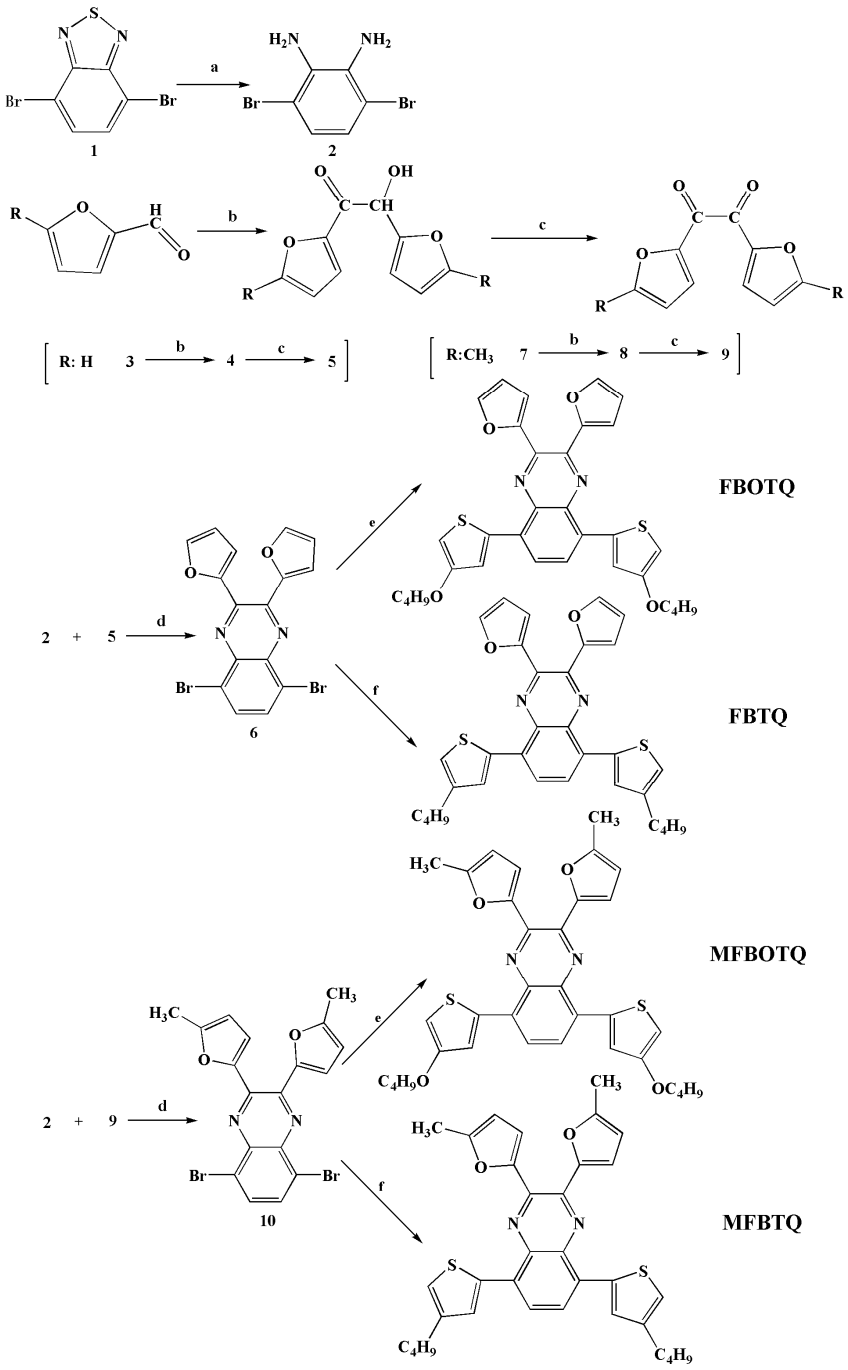


**Scheme 1** Synthetic route of the monomers. (a) $NaBH_4$, EtOH, 0 □, 24 h (b) vitamin B1, NaOH, EtOH (c) $CuSO_4 \cdot 5H_2O$, pyridine, reflux, 2.5 h (d) PTSA, EtOH, reflux, overnight (e-f) $Pd(PPh_3)_2Cl_2$, tributyl(2-(4-butoxythiophene))stannane (e), tributyl(2-(4-butylthiophene))stannane (f), dry THF, reflux, 24h.

ml of anhydrous ethyl alcohol were added into round-bottom flask, meanwhile, 16.5 g (436 mM) of $NaBH_4$ was added in three installments gradually. The solution was stirred in ice bath at 0 °C for 48 h. After the reaction, the mixture was pulled into distilled water, stirring and filtering to get white 3,6-dibromo-1,2-phenylenediamine solid.[34] The condensation reaction of 3,6-dibromo-1,2-phenylenediamine (1.33 g, 5 mmol) and 1,2-di(2-furyl) ethanedione[35] (0.95 g, 5 mmol) with 1:1 stoichiometric ratio afforded 2,3-bis(2-furyl)-5,8-dibromoquinoxaline with catalytic amounts of p-toluene sulfonic acid (PTSA) in EtOH (50 mL). The mixture was stirring magnetically overnight when refluxed. Cloudy mixture was achieved at the end of the reaction. Then solution was cooled to 0 °C and filtered. The separated solid was washed with EtOH several times and dried under vacuum oven to give a yellow-green 2,3-bis(2-furyl)-5,8-dibromoquinoxaline (**6**) powder (1.8 g, 85.7%). $^1$H NMR (400 MHz, $CDCl_3$, $Me_4Si$): δ 7.88 (2H, s, Ar H),

7.63 (2H, d), 6.97 (2H, d), 6.60 (2H, q). $^{13}$C NMR (101 MHz, $CDCl_3$, $Me_4Si$): δ 150.67, 145.14, 143.17, 139.10, 133.49, 123.59, 114.91, 112.45. (see Supporting Information Fig. S1†) A yellow solid of 2,3-bis(5-methylfuran-2-yl)-5,8-dibromoquinoxaline (**10**) was obtained by using condensation reaction of 3,6-dibromo-1,2-phenylenediamine (1.33 g, 5 mmol) and 1,2-di(5-methylfuran-2-yl) ethanedione[35] (1.09 g, 5 mmol)) under the same conditions in a good yield (1.86 g, 83%). $^1$H NMR (400 MHz, $CDCl_3$, $Me_4Si$): δ 7.82 (2H, s, Ar H), 6.93 (2H, d), 6.20 (2H, d), 2.41(6H, s). $^{13}$C NMR (101 MHz, $CDCl_3$, $Me_4Si$): δ 155.55, 149.21, 143.16, 138.88, 132.98, 123.38, 116.33, 108.87, 14.16. (see Supporting Information Fig. S2†)

### 2.3.2 General procedure for the synthesis of FBOTQ, FBTQ, MFBOTQ, MFBTQ

As shown in scheme 1, FBOTQ, FBTQ, MFBOTQ and MFBTQ were synthesized by Stille cross coupling reaction. Tributylstannane compounds were prepared following the literature method.[36] 2,3-bis(2-furyl)-5,8-dibromoquinoxaline (1.68 g, 4 mmol) or 2,3-bis(5-methylfuran-2-yl)-5,8-dibromoquinoxaline (1.792 g, 4 mmol) with the excessive corresponding tributylstannane compounds (16 mmol) using $Pd(PPh_3)_2Cl_2$ (0.28 g, 0.4 mmol) as the catalyst was dissolved in dry anhydrous THF (60 mL)at room temperature. The solution was stirred under nitrogen atmosphere for 30 min. Raise the temperature immediately until the solution was refluxed. The mixture was stirred under the above conditions for 24 h, then cooled and concentrated on the rotary evaporator. At the end, the mixture was purified by using column chromatography on silica gel with n-hexane-dichloromethane as the eluent.

**2,3-Di(2-furyl)-5,8-bis(2-(4-butoxythiophene)) quinoxaline (FBOTQ).** The crude mixture was chromatographed on silica gel by eluting with n-hexane: dichloromethane (3:1, by volume) to achieve FBOTQ as red solid (1.65 g, 72.4%). $^1$H NMR (400 MHz, $CDCl_3$, $Me_4Si$): δ 8.00 (2H, s, Ar H), 7.60 (2H, d), 7.57 (2H, d), 7.10 (2H, d), 6.61 (2H, dd), 6.45 (2H, d), 4.03 (4H, t), 1.81 (4H, m), 1.53 (4H, m),1.00 (6H, t). $^{13}$C NMR (101 MHz, $CDCl_3$, $Me_4Si$): δ 157.69, 151.69, 144.36, 140.50, 137.13, 130.82, 126.90, 119.00, 114.09, 112.18, 109.96, 101.64, 70.02, 31.52, 19.44, 14.00 (see Supporting Information Fig. S3†).

**2,3-Di(2-furyl)-5,8-bis(2-(4-butylthiophene)) quinoxaline (FBTQ).** The crude mixture was chromatographed on silica gel by eluting with n-hexane: dichloromethane (8:1, by volume) to obtain FBTQ as bright red-orange solid (1.68 g, 78.1%). $^1$H NMR (400 MHz, $CDCl_3$, $Me_4Si$): δ 8.05 (2H, s, Ar H), 7.77 (2H, s), 7.60 (2H, s), 7.11 (4H, d), 6.61 (2H, m), 2.70 (4H, t), 1.71 (4H, m), 1.44 (4H, m), 0.97 (6H, t). $^{13}$C NMR (101 MHz, $CDCl_3$, $Me_4Si$): δ 151.84, 144.27, 143.10, 140.37, 138.47, 136.97, 131.16, 128.56, 127.22, 123.80, 113.92, 112.16, 32.91, 30.42, 22.58, 14.12 (see Supporting Information Fig. S4†).

**2,3-Di(5-methylfuran-2-yl)-5,8-bis(2-(4-butoxythiophene)) quinoxaline (MFBOTQ).** The crude mixture was chromatographed on silica gel by eluting with n-hexane: dichloromethane (3:1, by volume) to give MFBOTQ as dark red solid (1.76 g, 73.6%). $^1$H NMR (400 MHz, $CDCl_3$, $Me_4Si$): δ 7.96 (2H, s, Ar H), 7.62 (2H, d), 7.04 (2H, d), 6.43 (2H, d), 6.21 (2H, dd), 4.03 (4H, t), 2.41 (6H, s), 1.80 (4H, m), 1.53 (4H, m),1.00 (6H, t). $^{13}$C NMR (101 MHz, $CDCl_3$, $Me_4Si$): δ 157.74, 154.63, 150.15, 140.49, 137.51, 136.88, 130.63, 126.48, 119.06, 115.55, 108.61, 101.34, 69.99, 31.60, 19.51, 14.10, 13.81(see Supporting Information Fig. S5†).

**2,3-di(5-methylfuran-2-yl)-5,8-bis(2-(4-butylthiophene)) quinoxaline (MFBTQ).** The crude mixture was chromatographed on silica gel by eluting with n-hexane: dichloromethane (8:1, by volume) to give MFBTQ as bright red solid (1.8 g, 79.5%).$^1$H NMR (400 MHz, $CDCl_3$, $Me_4Si$): δ 7.99 (2H, s, Ar H), 7.82 (2H, d), 7.08 (2H, s), 7.03 (2H, d), 6.20 (2H, dd), 2.69 (4H, m), 2.40 (6H, s), 1.70 (4H, m), 1.43 (4H, m), 0.96 ( 6H, t). $^{13}$C NMR (101 MHz, $CDCl_3$, $Me_4Si$): δ 154.50, 150.30, 143.19, 140.36, 138.85, 136.82, 130.97, 128.70, 126.85, 123.48, 115.37, 108.59, 33.00, 30.56, 22.70, 14.16 (see Supporting Information Fig. S6†).

## 3. Results and discussion

### 3.1 Synthesis of monomers

The synthetic route to the monomers is shown in Scheme 1. For a start, 4,7-dibromo-2,1,3-benzothiadiazole (**1**) was reduced by $NaBH_4$ as presented in the established literature procedures and then gave expected 3,6-dibromo-1,2-phenylenediamine (**2**).[34] The benzoin condensation of furfural (**3**) gave the desired 2-hydroxy-1,2-di(2-furyl) ethanone (**4**).[37] The synthetic route of 2-hydroxy-1,2-di(5-methylfuran-2-yl) ethanone (**8**)[37] was the same with that of **4**. 2-hydroxy-1,2-di(2-furyl) ethanone (**4**) and $CuSO_4{\cdot}5H_2O$ were added to a solution of distilled water and pyridine, and then oxidation of **4** obtained desired yellow acicular crystal 1,2-di(2-furyl) ethanedione (**5**).[35] Using the identical methods, 1,2-di(5-methylfuran-2-yl) ethanedione (**9**)[35] was achieved. The next, typical condensation reactions of **2** with 1,2-dione(**5**, **9**) respectively afforded the corresponding 2,3-bis(2-furyl)-5,8-dibromoquinoxaline (**6**) and 2,3-bis(5-methylfuran-2-yl)-5,8-dibromoquinoxaline (**10**). Ultimately, Stille coupling reactions of condensation product **6** with the corresponding tributylstannane compounds in the presence of $Pd(PPh_3)_2Cl_2$ as catalyst in dry THF gave the target monomers FBOTQ and FBTQ in satisfied yields (72-80%). Similarly, the target monomers MFBOTQ and MFBTQ obtained by using Stille coupling reaction in morderate yields (73-80%).

### 3.2 Electrochemistry

#### 3.2.1 Electrochemical polymerization

The electrochemical properties of monomers and their polymers were investigated by using cyclic voltammetry (CV). All four

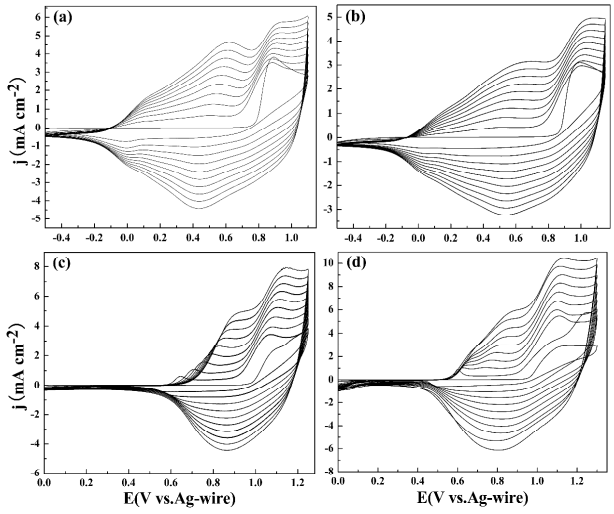

**Fig. 1** Cyclic voltammogram curves of FBOTQ (a), MFBOTQ (b), FBTQ (c) and MFBTQ (d) in ACN/DCM (1:1) containing 0.2 M $TBAPF_6$ solutions at a scan rate of 100 mV $s^{-1}$.

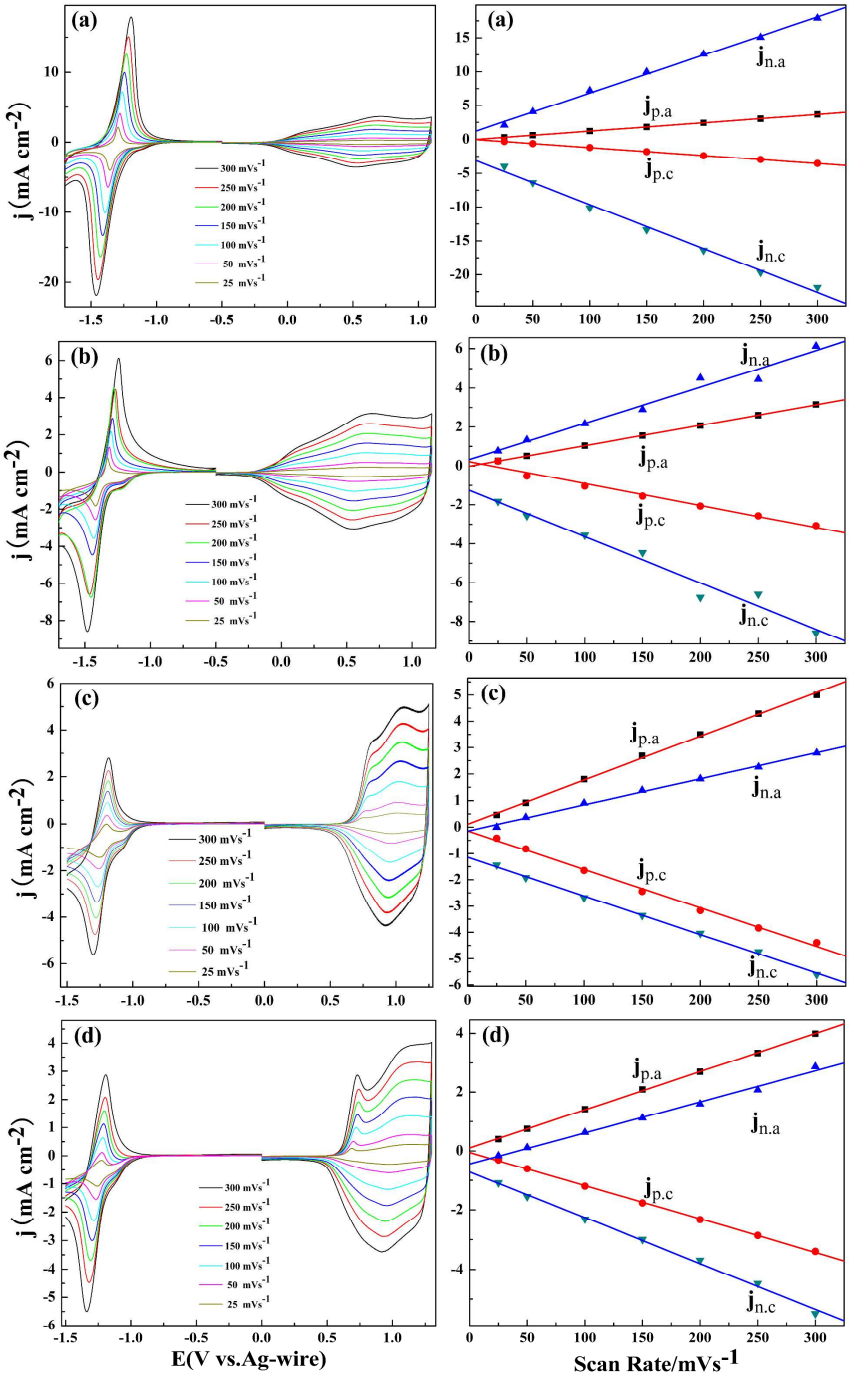


**Fig. 2** Left: CV curves of the PFBOTQ (a), PMFBOTQ (b), PFBTQ (c) and PMFBTQ (d) films at different scan rates between 25 and 300 mV $s^{-1}$ in the monomer-free 0.2 M $TBAPF_6$/ACN/DCM solution. Right: Scan rate dependence of the anodic and cathodic peak current densities graph of the p-doping/dedoping process and n-doping/dedoping process for the four polymer films.

polymers were deposited on Pt wire by cyclic voltammetry (CV) with the same potential scan rate (100 mV $s^{-1}$) in acetonitrile (ACN)/dichloromethane (DCM) (1:1, by volume) solvent mixture containing 0.2 M tetrabutylammonium hexafluorophosphate ($TBAPF_6$) as the supporting electrolyte and 0.005 M monomers. The successive CV curves of FBOTQ, MFBOTQ, FBTQ and MFBTQ were illustrated in Fig. 1. The first cycle of CV experiment depicted irreversible oxidation of the monomer. The onset oxidation potential ($E_{onset}$) of FBOTQ is 0.78 V and that of MFBOTQ, FBTQ and MFBTQ are 0.86 V, 0.98 V and 0.96 V, respectively. By contrast, the $E_{onset}$ of FBOTQ is far lower than that of FBTQ and similarly the $E_{onset}$ of MFBOTQ is also lower than that of MFBTQ due to the effect of strong electron-rich butoxythiophene group on donor moiety. Meanwhile, by comparing the $E_{onset}$ of FBOTQ with that of

MFBOTQ, it was clearly found that the onset oxidation potentials of the monomers with the identical donor were a bit different owning to the effect of methyl substituent on acceptor moiety. Analogously, the phenomenon also can be observed from the comparison between FBTQ and MFBTQ. There are usually two onset oxidation potentials for the CV curves of the monomers. The first oxidation peak of monomers might be related with the formation of the radical cation transition state, and the second onset potential was related with the formation of the radical cation, which led to the coupling reactions and the formation of polymers. Different with that of three other monomers, a positive shift was observed on the first potentials in the potenthiodynamic electrochemical polymerization of FBTQ (Fig. 1c) after several scans, the reason for which may be that pt electrode might have a catalytic effect on the formation of the radical cation transition state, and the cover of the electrode by the as-formed polymer impaired the catalytic effect, which could be compensated by the positive shift of the onset potentials. During the repetitive anodic potential scan of monomers, the new redox couples as well as concomitant increase in the current intensities implied that the corresponding electroactive polymer films were formed on the surface of working electrodes.[38]

### 3.2.2 Electrochemistry behaviors of the polymer films

Four polymer films were prepared on Pt wires by sweeping the potentials three cycles so as to investigate the electrochemical behaviors at different scan rates between 25 and 300 mV $s^{-1}$ in monomer free electrolyte solution. The left column of Fig. 2(a) demonstrated the electrochemical behavior of the PFBOTQ film at different scan rates from 25 to 300 mV $s^{-1}$ in acetonitrile (ACN)/dichloromethane (DCM) (1:1, by volume) solvent mixture containing 0.2 M tetrabutylammonium hexafluorophosphate ($TBAPF_6$). It was clearly observed that there was a couple of redox peaks with an oxidation potential of 0.71 V and a reduction potential of 0.51 V in the p-doping process. The sharp quasi-reversible redox peaks with an oxidation potential of -1.19 V and a reduction potential of -1.46 V was also observed in the reduction region, which demonstrated the conducting polymer had the character of n-doping. Furthermore, it was notable that the redox peaks of the n-doping/dedoping were much stronger than the p-doping/dedoping process. The results indicated that 2,3-bis(2-furyl)-5,8-dibromoquinoxaline (**6**) was a strong electron acceptor and PFBOTQ was a good n-type conjugated polymer.[39] The similar phenomenon of n-doping/dedoping process was observed from the other ploymers including PMFBOTQ, PFBTQ and PMFBTQ in Fig. 2. In contrast, both PFBOTQ and PMFBOTQ polymers presented a couple of redox peaks, respectively, while other polymers including PFBTQ and PMFBTQ exhibited two oxidation peaks and one reduction peak in p-doping process. The different appearances and different locations of the oxidation and reduction peaks of the polymers implied the influences which were made by different electron-rich groups as well as different acceptor units.

In addition, the $E_{onset}$ parameters of PFBOTQ, PMFBOTQ, PFBTQ and PMFBTQ were listed in Table 1. The parameters of PMFMQ and PMFTQ[32] were also listed in Table 1 in order to compare with the newly synthetic polymers. It can be easily found that the onset oxidation potentials of PFBOTQ and PMFBOTQ were a bit higher than that of PMFMQ, which indicated that the increase of alkyl chain length of alkoxy substituent on thiophene moiety slightly enhanced the electron-donating ability of donor unit but increased repulsive steric effect on neighboring repeat unit obviously and then led to a little higher onset potentials. Analogically, compared with PMFTQ, PFBTQ and PMFBTQ presented a little higher onset potentials due to that the weak electron-donating effect of the butyl group on thiophene ring can not compensate for its repulsive steric effect on neighboring repeat unit.

During the p-doping/dedoping process and the n-doping/dedoping process, a good linear relationship between the peak current density and scan rate of the PFBOTQ polymer was shown in the right column of Fig. 2(a), which directly demonstrated that a good electroactive polymer film was well adhered on ITO and the electrochemical process was non-diffusion-limited even at very low and high scan rates.[40] As expected, the similar linear relationship between the peak current density and scan rate of the other three polymers (PMFBOTQ, PFBTQ and PMFBTQ) was presented (Fig. 2).

### 3.2.3 Stabilities of the polymer films

The long-term switching stability between oxidized and neutral states is a severe requirement for electrochromic polymers, since these materials have a potential use in commercial devices.[41] In order to investigate the stabilities of the polymer films, four polymer films were prepared on Pt wires by sweeping the potentials five cycles at 100 mV $s^{-1}$ in the monomers saturated solution (ACN and DCM as solvent mixture, 1:1, by volume) containing 0.2 M $TBAPF_6$. The four as-prepared polymers were cycled 1000 times at 200 mV $s^{-1}$ in 0.2 M $TBAPF_6$/ACN/DCM solution, respectively. The charge involved during the electrochemical process was calculated for each voltammogram from the integration of current. The Fig. 3 showed the changes of CV curves for PFBOTQ, PMFBOTQ, PFBTQ and PMFBTQ films between the 1st and 1000th cycles. As shown in Fig. 3a, the total charge loss during electrochemical process was less than 5.3% between the initial and 1000th cycles for PFBOTQ films. It was noteworthy that most of this decrease happened during the first 500 cycles of CV curves, but the PFBOTQ film presented an immense stability with scarcely any charge loss (less than 1%) between the 500th and 1000th cycles. We did not proceed with further cycling since about 95% of the charge remained intact after 1000 cycles. The above result demonstrated that PFBOTQ film had an excellent stability in switching between doped and neutral states, which made it a good candidate for electrochromic device applications. Meanwhile, the overall charge loss for PMFBOTQ, PFBTQ and PMFBTQ films during this experiment were less than 8.7%, 11.7% and 12.1% between the original and 1000th cycles, respectively. From the stability measurements of PMFBOTQ, PFBTQ and PMFBTQ films, the similar phenomena were easily

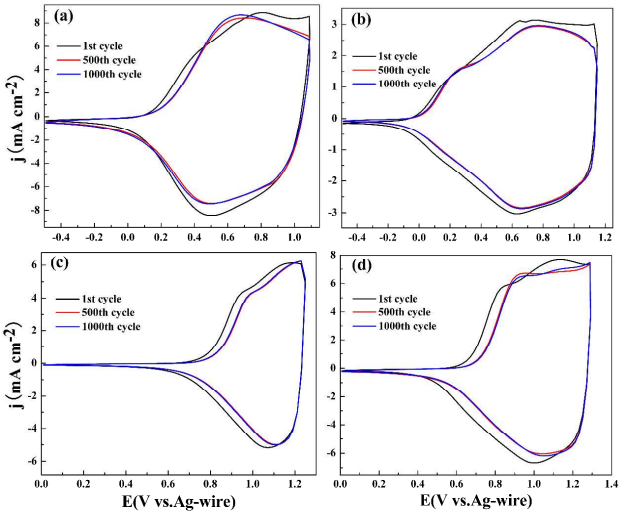

**Fig. 3** Stabilities of the PFBOTQ (a), PMFBOTQ (b), PFBTQ (c) and PMFBTQ (d) films cycled 1000 times with a scan rate of 200 mV $s^{-1}$ in the monomer-free 0.2 M $TBAPF_6$/ACN/DCM solution.

found that the main loss happened during the first 500 cycles and no significant charge reduction (less than 1%) was found between the 500th and 1000th cycles. Another phenomenon can also be observed that the PFBOTQ and PMFBOTQ polymer films containing butoxy group in thiophene derivative moiety presented much more stable than PFBTQ and PMFBTQ polymer films containing butyl group in thiophene derivative moiety. Furthermore, the total charge loss of each polymer film was less than 12.1% between the 1st and 1000th cycles, we concluded that the four polymer films presented superb stabilities, which made them potential applications in various fields, such as displays.[42]

### 3.3 Morphology

Scanning electron micrographs (SEM) of polymers provide their clear surface and bulk morphologies, which are closely related to their optical and electrical properties. Fig. 4 gave the SEM images of PFBOTQ, PMFBOTQ, PFBTQ and PMFBTQ, which were prepared potentiostatically in the ACN/DCM (1:1, by volume) solution containing 0.2 M $TBAPF_6$ and 0.005 M relevant monomers on ITO electrode. All the polymers were dedoped before characterization. As shown in Fig. 4a, there are lots of globules evenly distributed and each of the globules has the similar size with average diameter of around 1 um. Meanwhile, some pores and gaps are easily observed between the globules. As for PMFBOTQ film

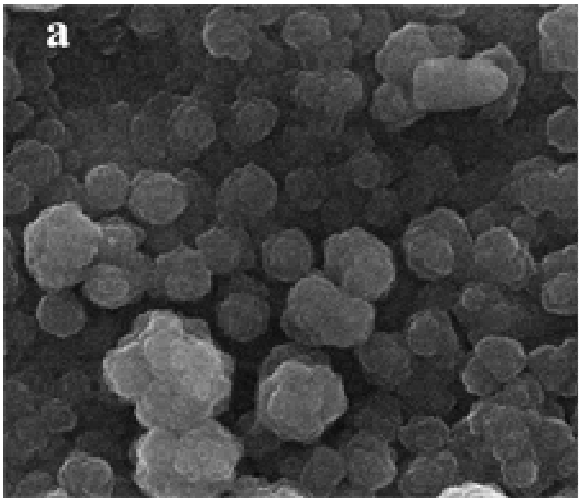


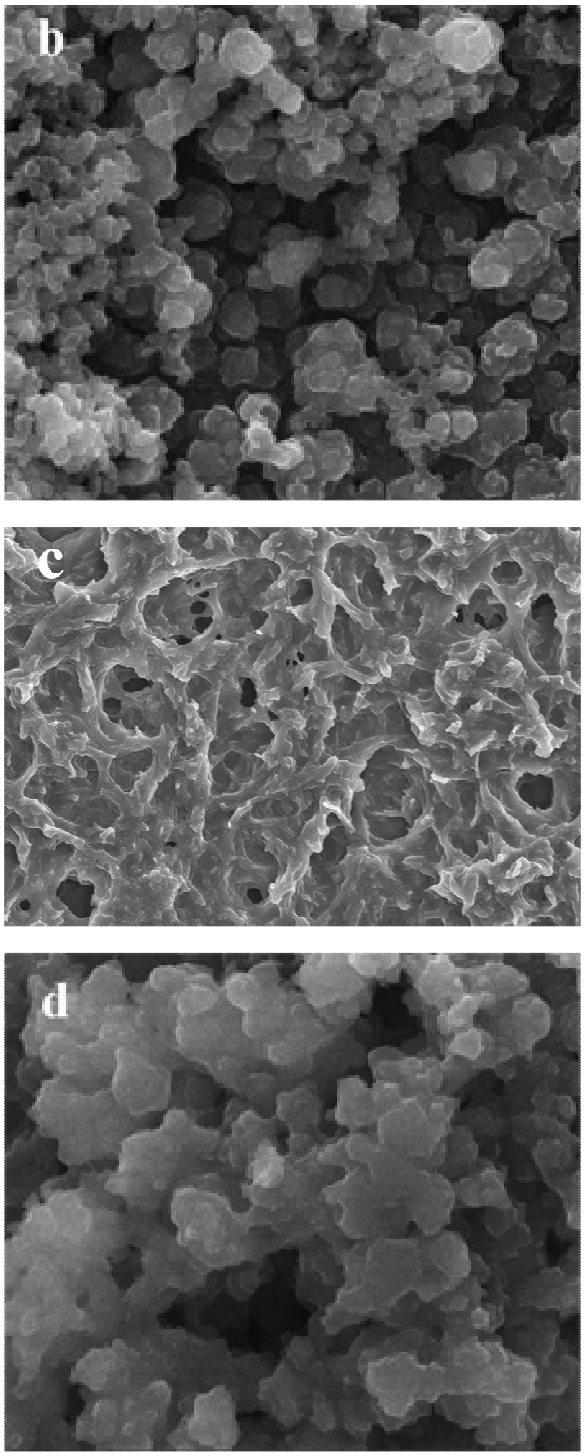


**Fig. 4** SEM images of PFBOTQ (a), PMFBOTQ (b), PFBTQ (c) and PMFBTQ (d) films deposited potentiostatically onto ITO electrode. Measurments of all SEM images were carried on at the same conditions and the scale of all SEM images with the same size is ×20.0k.

(Fig. 4b), it presents an accumulation state of small globular granules with interlinked holes among the clusters on the surface. With regard to PFBTQ film (Fig. 4c), it shows laminated structure with significant gibbosities and potholes pervading on the surface and some scattered holes are also found on the film. The PMFBTQ film

reveals an accumulation state of snowflake lamellar structures with lots of holes between the snowflake clusters. These morphologies facilitate the movement of doping anions into and out of the polymer film during doping and dedoping process, which has a great influence on the optical and electrical properties of polymer films.

Beside, step profiler measurements were carried on in order to study the thickness and surface roughness of the polymer films. The thickness for PFBOTQ, PMFBOTQ, PFBTQ and PMFBTQ films are about 1100 nm, 800 nm, 1300 nm and 1400 nm, respectively (see Supporting Information Fig. S7†). The images of step profiler measurements reveal that the polymer films have extremely rough surface with detective pits, which is in good agreement with morphologies of SEM images.

### 3.4 Optical properties of the monomers and films

The UV-Vis absorption spectra of four monomers (FBOTQ, MFBOTQ, FBTQ and MFBTQ) dissolved in $CH_2Cl_2$ and the corresponding dedoped polymer films which were deposited on ITO electrode were examined. And the optical properties of these novel monomers and films were analyzed. As the Fig. 5 presented, all four monomers exhibited two characteristic absorption bands as the typical feature of donor-acceptor conjugated compounds, which were assigned to the π-π* transition as well as intramolecular charge

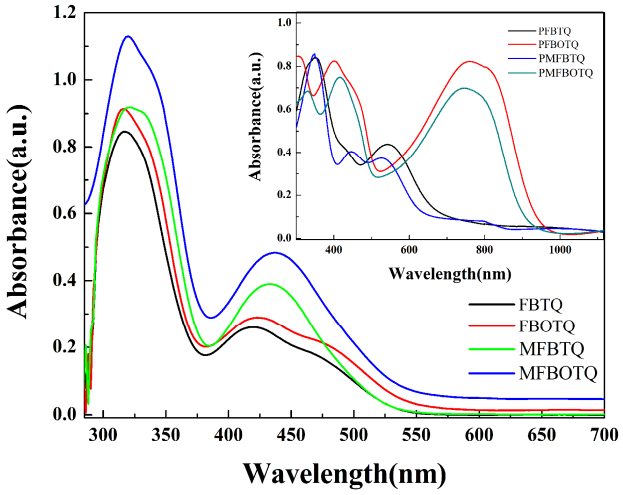


**Fig. 5** UV-Vis absorption spectra of FBOTQ, MFBOTQ, FBTQ and MFBTQ. Inset: absorption of the corresponding polymers in the neutral state.

transfer, respectively. As can be seen from Fig. 5, two obvious absorption peaks were observed at 316 and 424 nm for FBOTQ, 320 and 436 nm for MFBOTQ, around 316 and 420 nm for FBTQ as well as 321 and 432 nm for MFBTQ, respectively. Meanwhile, the optical band gaps ($E_g$) of the four monomers were calculated precisely from its low energy absorption edges ($\lambda_{onset}$) ($E_g$ = 1241/$\lambda_{onset}$). The $E_g$ of FBOTQ, MFBOTQ, FBTQ and MFBTQ monomers were calculated as 2.27 eV, 2.32 eV, 2.31 eV and 2.40 eV, respectively. Compared with FBTQ, FBOTQ had a little red shift of the low-energy absorption band and a lower band gap due to the strong electron-donating butoxy group on thiophene moiety which increased the conjugation effect of the D-A-D compound effectively. From the comparison between MFBTQ and MFBOTQ, the similar phenomenon was also seen easily. Besides, the $E_g$ of MFBOTQ was a slightly larger than that of FBOTQ on account of the influence of methyl group on acceptor moiety which decreased the electron-accepting ability of the acceptor unit. Similarly, the phenomenon above also can be observed from the contrast between FBTQ and MFBTQ.

Furthermore, the density functional theory (DFT) calculations were carried out on the DFT level employing the Gaussian 03 programs. The ground-state electron density distribution of the highest occupied molecular orbital (HOMO) and lowest unoccupied molecular orbital (LUMO) are illustrated in Fig. 6. In all four monomers, the HOMO and LUMO of orbital largely delocalized on the aromatic rings, which fully revealed that the newly-obtained compounds had the planar π-conjugated systems. And the system of D-A type can effectively lower the HOMO-LUMO gaps of corresponding polymers with enhanced planarity and higher electrical conductivity. Calculated HOMO-LUMO gap was found to be in the range 2.7-2.81 eV and the data were summarized in Table 1. The highest band gap was observed for MFBTQ and the lowest was for FBOTQ. These values were found to be nearly 0.41-0.45 V higher than the values from experimental data. This is mainly due to various effects such as solvent effects and to variation in solid state to the gaseous states. Even so, the relatively energy order of the calculated HOMO-LUMO gaps for all four polymers is in a good accordance with that of the experimental data.

The UV-Vis absorption spectra of the four neutral state films (PFBOTQ, PMFBOTQ, PFBTQ and PMFBTQ) prepared on ITO electrode were shown in the inset of Fig. 5. Both PFBOTQ and PMFBOTQ presented two obvious absorption peaks in visible region which were assigned to the strong π–π* transition and intramolecular charge transfer at neutral state, with the absorption peaks located at 402 nm and 758 nm for PFBOTQ and situated at 416 nm and 746 nm for PMFBOTQ. And a well-defined valley was observed at around 500 nm for both polymers, which gave rise to a valuable neutral green color. Different from PFBOTQ and PMFBOTQ, PFBTQ and PMFBTQ films showed two absorption peaks, with one maximum absorption peak at 349 nm in the UV region and another shoulder peak at 541 nm in the visible region for PFBTQ film and the two absorption peaks centered at 349 nm as well as around 500 nm for PMFBTQ film. Furthermore, the $E_g$ of four polymers (PFBOTQ, PMFBOTQ, PFBTQ and PMFBTQ) were calculated to be 1.32 eV, 1.37 eV, 1.85 eV and 1.95 eV, respectively. The band-gap is the difference in energy $E_g$ between the valence band and conduction band. Generally, the HOMO of the donor contributes to the polymer's valence band, and the LUMO of the acceptor contributes to the polymer's conduction band in D-A-D systems. As shown in Table 1, the introduction of the butoxy group on the thiophene moiety (donor unit) increased the HOMO levels of PFBOTQ and PMFBOTQ compared with their butyl-substituted homologue polymers, which then led to the lower band-gaps of the two polymers. The electron-donating abilities of alkoxy substituents are stronger than that of the alkyl substituents. In this case, the stronger are the electron-donating abilities of the substituent on the donor unit, the more profound conjugation effects are present on the polymers.

Compared with PFBTQ, PFBOTQ has an apparent red shift of the low-energy absorption wavelengths, which is in accordance with the decrease of its optical band gap. The similar phenomenon can be observed from the comparison of PMFBTQ and PMFBOTQ. The introduction of the methyl group on acceptor unit decreased the electron-accepting ability of the acceptor unit and increased repulsive steric effect on neighboring repeat unit as well as slightly increased the LOMO level of PMFBTQ and PMFBOTQ compared with their non-methyl substituted homologue polymers, which finally brought about the decrease of effective conjugation length in

the homopolymers[43] and a bit higher band-gaps of the two polymers. Moreover, all four polymers exhibit a bathochromic shift compared to the corresponding monomers as depicted in the inset of Fig. 5, which clearly demonstrate the formation of the long conjugated polymer chains due to the fact that the longer wavelength is the absorption, the higher conjugation length is the polymer.[44]

By contrast, the optical band gaps of PFBOTQ and PMFBOTQ was somewhat higher than that of PMFMQ[32] film owing to that the dominant stereo-hindrance effect of butoxy-substituent on donor unit decreased the conjugation length in homopolymers. Similarly, this can also explain the fact that PFBTQ and PMFBTQ had a slightly larger band gaps than that of PMFTQ.[32]

Table 1 clearly summarized the experimental parameters (the onset oxidation potential ($E_{onset}$), maximum absorption wavelength ($\lambda_{max}$), onset of the optical absorption spectra ($\lambda_{onset}$), optical band gap ($E_g$), HOMO and LUMO energy levels) of the monomers and the corresponding polymers for p-type doping. HOMO energy levels of the monomers and polymer films were calculated by using the

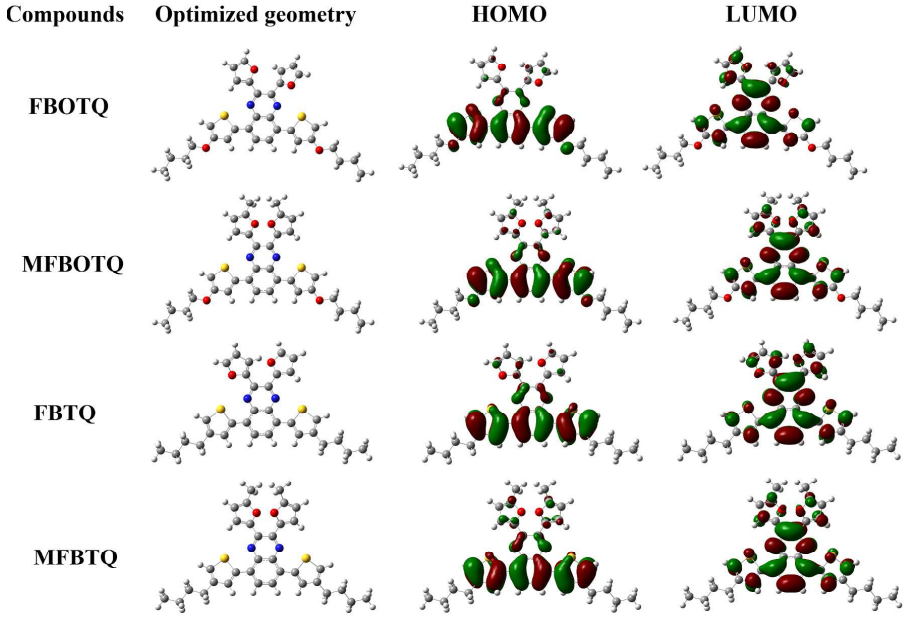


**Fig. 6** The optimized geometries and the molecular orbital surfaces of the HOMOs and LUMOs for the monomers obtained at the B3LYP/6-31G level.

**Table 1** The experimental parameters (onset oxidation potential ($E_{onset}$), maximum absorption wavelength ($\lambda_{max}$), onset of the optical absorption spectra ($\lambda_{onset}$), optical band gap ($E_g$[a]), HOMO/LUMO energy levels of the monomers and corresponding polymers) and the calculated data of the monomers from the Gaussian 03 programs.

| Compounds | $E_{onset}$,vs. (Ag-wire) (V) | $\lambda_{max}$ (nm) / $\lambda_{onset}$ (nm) | $E_g$[a] (eV) | HOMO[b] (eV) | LUMO[c] (eV) | $\Delta E$[d] | HOMO[d] (eV) | LUMO[d] (eV) |
|---|---|---|---|---|---|---|---|---|
| FBOTQ | 0.78 | 316,424/546 | 2.27 | -5.2 | -2.93 | 2.7 | -5.30 | -2.60 |
| MFBOTQ | 0.86 | 320,436/535 | 2.32 | -5.28 | -2.96 | 2.77 | -5.26 | -2.49 |
| FBTQ | 0.98 | 316,420/537 | 2.31 | -5.4 | -3.09 | 2.75 | -5.27 | -2.52 |
| MFBTQ | 0.96 | 321,432/518 | 2.40 | -5.38 | -2.98 | 2.81 | -5.24 | -2.43 |
| PFBOTQ | -0.18 | 402,758/939 | 1.32 | -4.24 | -2.92 | - | - | - |
| PMFBOTQ | -0.21 | 416,746/905 | 1.37 | -4.21 | -2.84 | - | - | - |
| PFBTQ | 0.66 | 349,541/670 | 1.85 | -5.08 | -3.23 | - | - | - |
| PMFBTQ | 0.62 | 349,500/638 | 1.95 | -5.04 | -3.09 | - | - | - |
| PMFMQ[e] | -0.18 | - | 1.22 | - | - | - | - | - |
| PMFTQ[e] | 0.48 | - | 1.65 | - | - | - | - | - |

[a] Calculated from the low energy absorption edges ($\lambda_{onset}$), $E_g = 1241/\lambda_{onset}$. [b] HOMO = $-e(E_{onset} + 0.02 + 4.4)$.

[c] Calculated by the addition of the optical band gap to the HOMO level. [d] Calculated by employing the Gaussian 03 programs.

[e] Data were taken from Ref.[32]

formula HOMO = $-e(E_{onset} + 0.02 + 4.4)$. Herein, the number 0.02 in the formula is a correction parameter due to the reference electrode used in the experiments is not standard electrode. So before and after each experiment, the silver pseudo reference was calibrated versus the ferrocene[47] redox couple and then adjusted to match the SCE reference potential. For ACN : DCM = 1:1 (v:v), the adjusted value is 0.02. The LUMO energy levels of them can also be calculated through the formula LUMO= HOMO+$E_g$.[45,46] And the calculated data from the Gaussian 03 programs of the monomers were also shown in Table 1.

### 3.5 Spectroelectrochemical properties of the polymer films

Spectroelectrochemistry is a available research method for obtaining the changes in the absorption spectra and the information about the electronic structures of conjugated polymers as a function of the applied potential difference.[48] In order to obtain the in-situ UV-Vis-NIR spectra, the PFBOTQ, PMFBOTQ, PFBTQ and PMFBTQ films were electrodeposited onto ITO electrode with the same polymerization charge of $2.0\times10^{-2}$ C under constant potential 1.1 V, 1.15V, 1.25 V and 1.3 V, respectively. In situ electronic absorption spectra of four polymer films were investigated upon stepwise oxidation in a monomer free 0.2 M $TBAPF_6$/ACN/DCM solution. As seen from Fig. 7, all four polymers exhibited two transitions due to their donor-acceptor nature at the neutral state. The two transitions in D-A-D type polymers were attributed to the transitions from the thiophene-based valence band to its antibonding counterpart (high-energy transition) and to the substituent-localized conduction band (low-energy transition). Hence, interactions between donor and acceptor units (their match) determined the energy and intensity of these transitions.[49] For PFBOTQ and PMFBOTQ, the intensities for high-energy transitions and low-energy transitions are comparable with each other, which indicates the ideal match between the donor and acceptor units and the strong interactions between them. Different with that of PFBOTQ and PMFBOTQ, the intensities of low-energy transitions for PFBTQ and PMFBTQ are substantially lower than that of the corresponding high-energy transitions, as observed from the shoulder-like absorption bands in the visible region.

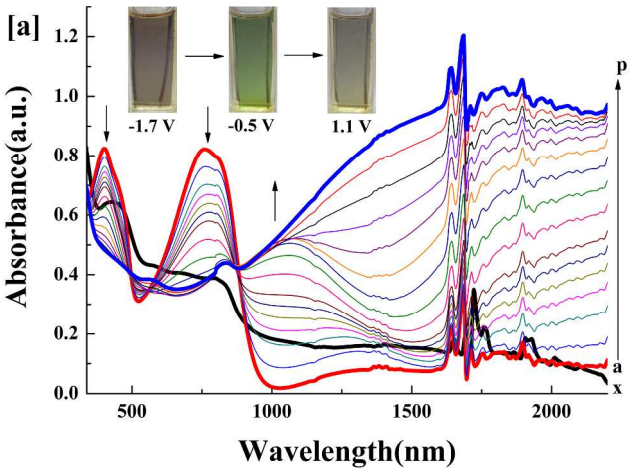


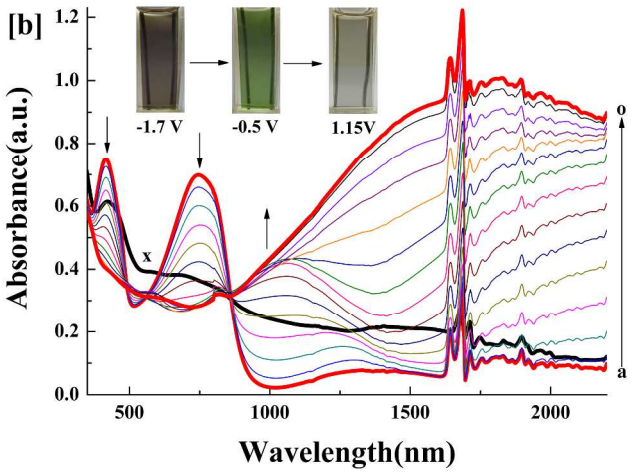


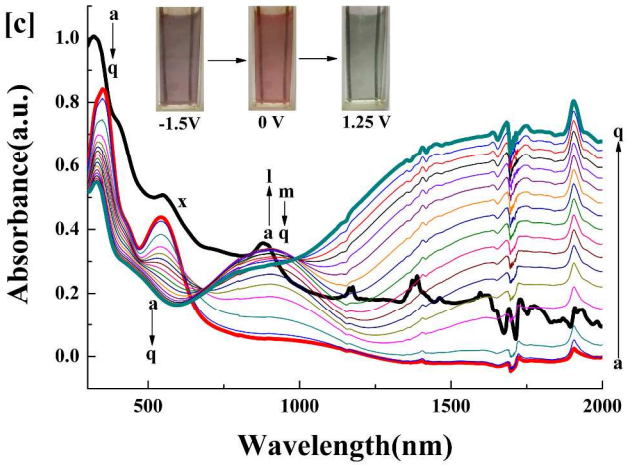


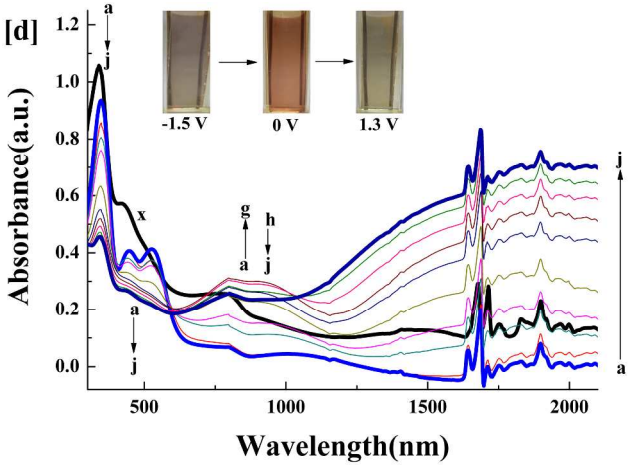


**Fig. 7** [a] p-doping: Spectroelectrochemistry of PFBOTQ film on ITO electrode in the monomer-free 0.2 M $TBAPF_6$/ACN/DCM solution at applied potentials: (a) -0.5, (b) -0.1, (c) 0.0, (d) 0.05, (e) 0.1, (f) 0.15, (g) 0.2 (h) 0.3, (i) 0.4, (j) 0.5, (k) 0.6, (l) 0.7, (m) 0.8, (n) 0.9, (o) 1.0, (p) 1.1 V. n-doping: Bold black line marked by 'x' indicates reduction spectra of PFBOTQ film at -1.7 V and the other two bold lines are the spectra of PFBOTQ film at -0.5 V (a) and 1.1 V (p), respectively. [b] p-doping: Spectroelectrochemistry of

PMFBOTQ film on ITO electrode in the monomer-free 0.2 M $TBAPF_6$/ACN/DCM solution at applied potentials: (a) -0.5, (b) -0.1, (c) 0.0, (d) 0.1, (e) 0.2, (f) 0.3, (g) 0.4 (h) 0.5, (i) 0.6, (j) 0.7, (k) 0.8, (l) 0.9, (m) 1.0, (n) 1.1, (o) 1.15 V. n-doping: Bold black line marked by 'x' indicates reduction spectra of PMFBOTQ film at -1.7 V and the other two bold lines are the spectra of PMFBOTQ film at -0.5 V (a) and 1.15 V (o), respectively. [c] p-doping: Spectroelectrochemistry of PFBTQ film on ITO electrode in the monomer-free 0.2 M $TBAPF_6$/ACN/DCM solution at applied potentials: (a) 0, (b) 0.5, (c) 0.55, (d) 0.6, (e) 0.65, (f) 0.7, (g) 0.75 (h) 0.8 (i) 0.85, (j) 0.9, (k) 0.95, (l) 1.0, (m) 1.05, (n) 1.1, (o) 1.15, (p) 1.20 and (q) 1.25 V. n-doping: Bold black line marked by 'x' indicates reduction spectra of PFBTQ film at -1.5 V and the other two bold lines are the spectra of PFBTQ film at 0 V (a) and 1.25 V (q), respectively. [d] p-doping: Spectroelectrochemistry of PMFBTQ films on ITO electrode in the monomer-free 0.2 M $TBAPF_6$/ACN/DCM solution at applied potentials: (a) 0, (b) 0.6, (c) 0.7, (d) 0.8, (e) 0.9, (f) 0.95, (g) 1.0, (h) 1.1, (i) 1.2, (j) 1.3 V. n-doping: Bold black line marked by 'x' indicates reduction spectra of PFBTQ film at -1.5 V and the other two bold lines are the spectra of PMFBTQ film at 0 V (a) and 1.3 V (j), respectively.

Upon oxidation of four polymers (PFBOTQ, PMFBOTQ, PFBTQ and PMFBTQ), formation of charge carriers such as polarons and bipolarons led to new absorption bands in NIR while absorptions for the neutral states were decreasing. In-situ spectroelectrochemical studies for the polymer films showed that the color of the film changed from green to highly transmissive near colorless hue for PFBOTQ and PMFBOTQ. Although there was a minor difference between the optical band gaps of PFBOTQ and PMFBOTQ, two polymer films revealed no apparent difference in color changes from neutral to oxidized states. UV-Vis spectra for PFBOTQ and PMFBOTQ which were shown in Fig. 7(a) and Fig. 7(b) displayed well-defined isosbestic points at approx. 870 nm and 860 nm respectively, indicating that PFBOTQ and PMFBOTQ polymers were being interconverted between two distinct forms on both occasions: the neutral form and radical cation. Spectroelectrochemical studies for PFBTQ film showed that the color of the film changed from light purplish red to transmissive slight gray color during oxidation. On the other hand, its 2,3-di(5-methylfuran-2-yl) substituted homologue PMFBTQ switched between light brown-red to slight brown-gray color, revealed less transmissive color than that of PFBTQ in the oxidized state since polaronic absorption bands tailed more into the visible region. The colors of four polymer films between neutral state and oxidation state changed from green or red to transmissive hue, which made them superior advantages in myriad of potential applications such as photovoltaic devices,[4] sensors[5] and smart windows.[8]

It is well known that only a fraction of the conjugated polymers can exhibit the property of n-doping on account of the easy degradation reaction associated with water and air.[50] For this reason, the conjugated polymers with stable negatively doped states are of high interest due to the widely applications such as LEDs and ambipolar field effect transistors. From the measurements of CV curves for the four polymer films, we preliminarily drawn the conclusion that the four polymers had the n-doping properties due to the reversible redox peaks in reduction region. But for further ascertain, the reductive UV-Vis absorption spectra of four polymers (PFBOTQ, PMFBOTQ, PFBTQ and PMFBTQ) were performed at -1.7, -1.7 , -1.5 and -1.5 V, respectively, in order to characterize the optical changes that occurred during the n-doped process and prove the introduction of charge carriers to the conjugated systems at n-doped state of four polymers. As shown in Fig. 7a, as the potential switched from the neutral state to the reduced state, several apparent changes have been observed for PFBOTQ, including the moderate absorption increase in the NIR region, the vanishment of the absorption band at around 758 nm, and the decrease accompanying with red-shift of the $\pi$-$\pi^*$ transition band. Meanwhile, the color of PFBOTQ film changed from green color to taupe color, which confirmed a true n-type doping process. A similar change was observed for the reduced state of PMFBOTQ, the absorption peak at 422 nm, and the less intense broad shoulder band between 542 nm and 845 nm resulted in a dark brown color at -1.7 V. As for PFBTQ, when the potential stepped from neutral sate (0 V) to the reduced state (-1.5 V), there was a uniform increase in the absorption of the polymer throughout the entire wavelength range with only a tiny peak centered at 548 nm in visible region, which brought about a slight purple color for the reduced PFBTQ. There is also an apparent difference between the absorption wavelengths of the neutral and reduced states of the PMFBTQ films. Upon reduction from the neutral state, the color of the PMFBTQ film was changed from light brown-red color to the light gray color, which was characterized by the separated absorption waves including a well defined band centered at 340 nm and a less intense shoulder absorption band centered at 418 nm. Hence, with strong absorption changes in the NIR region and the CV waves observed at negative potentials, it is clear that all of four polymers are revealing true n-type doping processes.

### 3.6 Switching properties of the polymer films

It is important that polymers can switch rapidly and present a prominent color change for electrochromic applications. Double potential step chronoamperometry technique coupled with optical spectroscopy was applied in order to investigate the switching ability of polymer film between its neutral and full oxidized state at definite wavelengths. The electrochromic switching behaviors of four polymer films were performed at regular intervals of 4 s in a monomer free ACN/DCM (1:1, by volume) solution containing 0.2 M $TBAPF_6$ as a supporting electrolyte. The stabilities, optical contrasts as well as response times based on electrochromic switching of four polymer films at different given wavelenghths were shown in Fig. 8. One of the crucial factors in appraising an electrochromic material is the optical contrast ($\Delta T$%), which can be defined as a percent transmittance change at a specified wavelength between the redox states. Meanwhile, another important characteristic parameter of electrochromic materials is the response time, which can be defined as the time required for reaching 95% of the full optical switch (after which the naked eye could not sense the color change).[51] Fig. 8(a) and Fig. 8(b) shows the switching properties of PFBOTQ and PMFBOTQ polymer films between -0.5 and 1.1 V for PFBOTQ as well as between -0.5 and 1.15 V for PMFBOTQ respectively at two different wavelengths both in visible and NIR regions. The optical contrast for PFBOTQ was calculated as 34.2% at 750 nm, 63.6% at 1810 nm and the switching times were 0.7 s at 750 nm as well as 1.1 s at 1810 nm from reduced to oxidized state. The percentage transmittance changes between the neutral (at -0.5 V) and oxidized states (at 1.15 V) were found to be 33% at 745 nm in the visible region as well as 66% at 1810 nm in the near-infrared region for PMFBOTQ polymer film. The response times of PMFBOTQ polymer film were 0.5 s at 745 nm and 0.9 s at 1810 nm from neutral state to oxidized state. As presented in Fig. 8(c), the dynamic electrochromic experiment for PFBTQ film was carried out at 545 nm, 900 nm and 2000 nm with potentials switched from 0 V to 1.25 V at regular intervals of 4s. The optical contrasts for PFBTQ were calculated to be 21% at 545 nm, 33% at 900 nm and 48.5% at 2000 nm. The response times of PFBTQ obtained by precise calculation were 0.7 s at 545 nm, 0.7 s at 900 nm as well as 1.3 s at 2000 nm from the reduced to the oxidized state.

With regard to PMFBTQ, it exhibited 24% transmittance change at 345 nm and 63% at 1970 nm between redox states in Fig. 8(d). Furthermore, switch times acquired were 0.9 s at 345 nm and 1.2 s at 1970 nm from the neutral to the oxidized state. By contrast, it can be easily found that PFBOTQ had better stability and higher percent transmittance contrast as well as faster switch time than that of PFBTQ. The similar conclusion can be drawn by comparison between PMFBOTQ and PMFBTQ. PFBOTQ and PMFBOTQ with the same butoxythiophene donor unit but different acceptors, presented the similar optical contrast, while PMFBOTQ polymer film showed a tiny bit faster switch time than that of PFBOTQ. Moreover, PFBOTQ and PMFBOTQ having excellent optical contrast in NIR region could be the better candidates for electrochromic display applications. By contrast, PMFBTQ showed higher optical contrast than PFBTQ, although switch times of the two polymers were different. As shown in Fig. 8, the electrochromic stabilities of the polymer films were investigated by using spectroelectrochemically kinetic studies (differentiated the transmittance changes after 1000 cycles). After 1000 cycles switching, four polymer films kept working without significant loss in their performance. The optical contrasts of PFBOTQ were

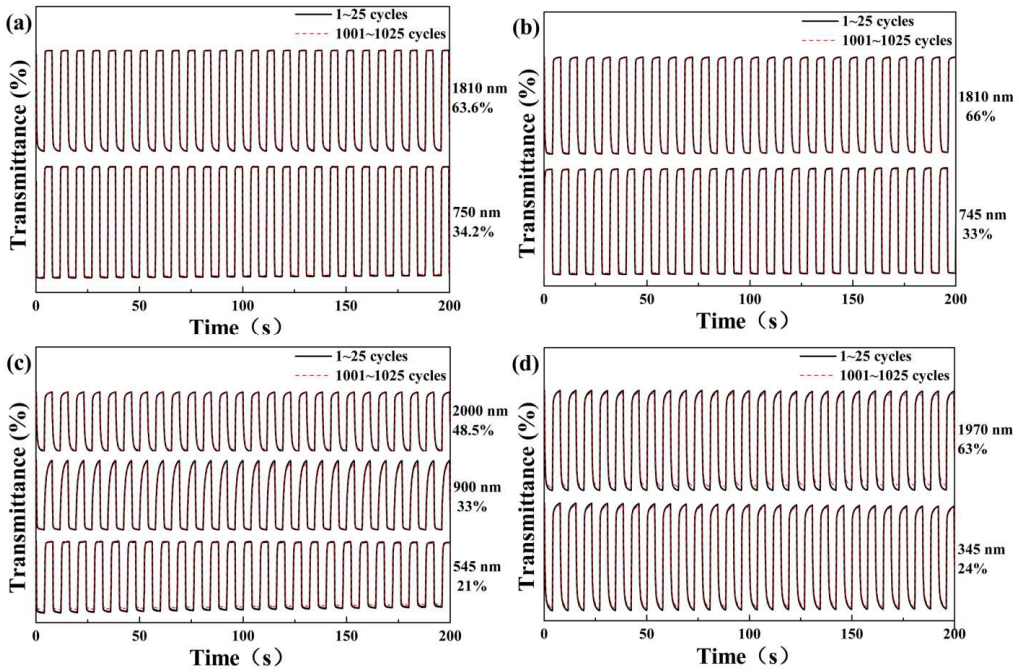


**Fig. 8** Transmittance-time profiles of the polymer films recorded during double-step spectrochronoamperometry for a switching time of 4 s under the indicated wavelength. (a) PFBOTQ between -0.5 and 1.1 V; (b) PMFBOTQ between -0.5 and 1.15 V; (c) PFBTQ between 0 V and 1.25 V; and (d) PMFBTQ between 0 V and 1.3 V.

**Table 2** The optical contrast ($\Delta T$%), response time, coloration efficiency (CE) and retained optical activity (after 1000 cycles, $\Delta$Y%) of the PFBOTQ, PMFBOTQ, PFBTQ and PMFBTQ.

| Compounds | λ (nm) | Optical contrast ($\Delta T$%) | Response time (s) | Coloration efficiency (CE, $cm^2\ C^{-1}$) | Retained optical activity (after 1000 cycles, $\Delta$Y% ) |
|---|---|---|---|---|---|
| PFBOTQ | 750 | 34.2 | 0.7 | 194.2 | 98.5 |
| | 1810 | 63.6 | 1.1 | 259.5 | 99.0 |
| PMFBOTQ | 745 | 33.0 | 0.5 | 220.9 | 97.8 |
| | 1810 | 66.0 | 0.9 | 227.7 | 98.0 |
| PFBTQ | 545 | 21.0 | 0.7 | 99.3 | 95.0 |
| | 900 | 33.0 | 0.7 | 378.4 | 94.3 |
| | 2000 | 48.5 | 1.3 | 360.3 | 96.5 |
| PMFBTQ | 345 | 24.0 | 0.9 | 215.7 | 94.6 |
| | 1970 | 63.0 | 1.2 | 353.2 | 93.5 |
| PMFMQ[a] | 428 | 22.0 | 0.9 | - | - |

| | | | | | |
|---|---|---|---|---|---|
| | 760 | 24.0 | 0.7 | - | - |
| | 1600 | 86.0 | 1.1 | - | - |
| | 560 | 18.0 | 1.6 | - | - |
| PMFTQ[a] | 790 | 60.0 | 1.4 | - | - |
| | 1300 | 80.0 | 1.6 | - | - |

[a] Data were taken from Ref.[32]

retained by 98.5% of its origination at 750 nm and 99.0% at 1810 nm, respectively, after 1000 cycles of the operation, which demonstrated that the PFBOTQ had excellent electrochromic stability in switching between the doped and neutral states. Meanwhile, the retained optical contrasts of PMFBOTQ, PFBTQ and PMFBTQ were shown in Table 2. From the data, it was readily observed that PFBOTQ and PMFBOTQ were much more stable than that of PFBTQ and PMFBTQ due to the effect of strong electron-rich butoxy group, which was in a good agreement with the result of the CV stabilities. And the total loss of the optical contrasts for each polymer film was less than 6.5% after 1000 cycles of operation, the conclusion can be drawn that the four polymers presented superb kinetic and redox stabilities.

Coloration efficiency (CE) is another key parameter for electrochromic polymer films as it describes the change in optical absorbance at the wavelength of interest to the density of injected/ejected charge.[52] CE at a given wavelength (λ) can be calculated by using the equations are given below:[53]

$$\Delta OD = \lg\left(\frac{T_b}{T_c}\right) \text{ and } \eta = \frac{\Delta OD}{\Delta Q}$$

where $T_b$ and $T_c$ are the transmittances before and after coloration at λ, respectively. ΔOD is the change of the optical density at λ, which is proportional to the amount of produced color centers. ΔQ is the amount of injected/ejected charge per unit sample area. $\eta$ denotes the coloration efficiency (CE) at a given wavelength (λ). The CE of PFBOTQ film was calculated to be 194.2 $cm^2\ C^{-1}$ at 750 nm and 259.5 $cm^2\ C^{-1}$ at 1810 nm. As for PMFBOTQ, the data of CE calculated by the equations mentioned above were 220.9 $cm^2\ C^{-1}$ at 745 nm and 227.7 $cm^2\ C^{-1}$ at 1810 nm. With regard to PFBTQ, the values of CE were measured as 99.3 $cm^2\ C^{-1}$ at 545 nm, 378.4 $cm^2\ C^{-1}$ at 900 nm and 360.3 $cm^2\ C^{-1}$ at 2000 nm by the same method. We also easily obtained the values of CE for PMFBTQ. The CE of PMFBTQ polymer were 215.7 $cm^2\ C^{-1}$ at 345 nm and 353.2 $cm^2\ C^{-1}$ at 1970 nm. It was clearly found that all of CE values for four polymer films were greater than or about 200 $cm^2\ C^{-1}$ except the CE value of PFBTQ at 545 nm. The newly synthesized four polymers exhibited excellent CE properties by comparison with the CE (in the range of 80-100 $cm^2\ C^{-1}$) of naphthalenediimide bridged D-A polymers[27] reported recently, which was due to the favorable matches (D-A interactions) of the four polymers. The results clearly showed that four polymer films had very satisfactory coloration efficiencies. From the analyses of the switching properties for the four polymer films, we can conclude that the high optical contrast, fast switching times and well-pleasing CE values make four polymer films good candidates for promising applications such as smart windows, electrochromic mirrors, optical displays and so on.

The parameters (optical contrasts, response times and the coloration efficiencies) of PFBOTQ, PMFBOTQ, PFBTQ and PMFBTQ were presented in Table 2. In addition, the parameters for PMFMQ and PMFTQ[32] were also listed for comparison. The previous experience was that long chain alkyl group of polymers can improve the optical contrasts and response times of polymers in some extent due to the increase of the distance between chain segments, which can enhance the charge and discharge capacity of anion in doping process. In this case, it is speculated that all of the four polymers in this study should present higher optical contrasts and faster response times than that of PMFMQ and PMFTQ. All four polymers present outstanding response times by contrast with that of PMFMQ and PMFTQ, which is agreement with the previous experience. Unexpectedly, the four newly synthetic polymers exhibit a little lower optical contrasts by comparison with that of PMFMQ and PMFTQ, which is inconsistent with the previous experience and the reason of this phenomenon will need to further study.

## 4. Conclusions

In summary, four novel donor-acceptor-donor type monomers based on 2,3-di(2-furyl) quinoxaline or 2,3-di(5-methylfuran-2-yl) quinoxaline as the acceptor units were successfully synthesized in order to study the effects of the different donor and different acceptor strengths on the electrochemical and spectroelectrochemical properties of the resulting electropolymerized materials. Electrochemical studies and spectroelectrochemical characterizations indicated that both PFBOTQ and PMFBOTQ with the stronger electron-donor butoxythiophene unit had lower oxidation potentials and band gaps relative to the polymers containing butylthiophene unit and PFBOTQ exhibited the lower oxidation potential and band gap compared to polymer PMFBOTQ due to the effect of methyl on quinoxaline moiety. In addition, both PFBOTQ and PMFBOTQ are exhibited to be neutral-state green polymeric materials.

As the D-A-D type of π-conjugated polymers, they all showed excellent cyclic voltammetry stabilities, satisfactory coloration efficiencies (CE), high optical contrasts (Δ*T*%) and extremely fast response times. What's more, generation of redox waves in CV curves at negative potentials and variation of the spectral absorption curves upon reduction proved that all four polymers had stable n-doping properties. The polymer films with their excellent electrochemical and optical properties, are expected to be useful for practical use in electrochromic display applications.

## Acknowledgements

The work was financially supported by the National Natural Science Foundation of China (51473074, 31400044), the General

and Special Program of the postdoctoral science foundation China (2013M530397, 2014T70861).

## Notes and references

Shandong Key laboratory of Chemical Energy Storage and Novel Cell Technology, Liaocheng University, Liaocheng, 252059, P.R. China
Correspondence to: Jinsheng Zhao (E-mail: j.s.zhao@163.com); Jifeng Liu (E-mail:liujifeng@lcu.edu.cn)

† Electronic Supplementary Information (ESI) available: $^{1}$HNMR and $^{13}$CNMR spectra of the intermediates and target compounds; the thickness tests of the polymers.

1 H. Shirakawa, E. J. Louis, A. G. Macdiarmid, C. K. Chinag and A. J. Heeger, *Chem. Commun*., 1977, **16**, 578.
2 J. H. Burroughes, D. D. C. Bradley, A. R. Brown, R. N. Marks, K. Mackay, R. H. Friend, P. L. Burns and A. B. Holmes, *Nature*, 1990, **347**, 539.
3 A. Bessiere, C. Duhamel, J. C. Badot, V. Lucas and M. C. Certiat, *Electrochim. Acta*, 2004, **49**, 2051.
4 N. S. Sariciftci, D. Braun, C. Zhang, V. Srdanov, A. J. Heeger, G. Stucky and F. Wudl, *App. Phys. Lett*., 1993, **62**, 585.
5 D. T. McQuade, A. E. Pullen and T. M. Swager, *Chem. Rev.*, 2000, **100**, 2537.
6 N. Stutzmann, R. H. Friend and H. Sirringhaus, *Science*, 2003, **299**, 1881.
7 C. Yang, J.Y. Kim, S. Cho, J. K. Lee, A. J. Heeger and F. Wudl, *J. Am. Chem. Soc.*, 2008, **130**, 6444-6450.
8 C. G. Granqvist, A. Azens, A. Hjelm, L. Kullman, G. A. Niklasson, D. Ronnow, M. S. Mattsson, M. Veszelei and G. Vaivars, *Sol. Energy*, 1998, **63**, 199.
9 P. Chandrasekhar, B. J. Zay, G. C. Birur, S. Rawal, E. A. Pierson, L. Kauder and T. Swanson, *Adv. Funct. Mater*., 2002, **12**, 95-103.
10 S. Beaupré, A. -C. Breton, J. Dumas and M. Leclerc, *Chem. Mater.*, 2009, **21**, 1504-1513.
11 M. E. Nicho, H. Hu, C. López-Mata and J. Escalante, *Sol. Energy Mater. Sol . Cells*, 2004, **82**, 105-118.
12 E. Sefer, F. B. Koyuncu, E. Oguzhan and S. Koyuncu, *J. Polym. Sci., Part A: Polym. Chem.*, 2010, **48**, 4419-4427.
13 A. A. Argun, A. Cirpan and J. R. Reynolds, *Adv. Mater*., 2003, **15**, 1338.
14 R. J. Mortimer, *Electrochim. Acta*, 1999, **44**, 2971.
15 P. R. Somani and S. Radhakrishnan, *Mater. Chem. Phys.*, 2002, **77**, 117.
16 G. Sonmez, H. B. Sonmez, C. K. F. Shen, R. W. Jost, Y. Rubin and F. Wudl, *Macromolecules*, 2005, **38**, 669.
17 E. K. Unver, S. Tarkuc, Y. A. Udum, C. Tanyeli and L. Toppare, *org. Electron.*, 2011, **12**, 1625.
18 Y. J. Cheng, S. H. Yang and C. S. Hsu, *Chem. Rev*., 2009, **109**, 5868.
19 G. E. Gunbas, A. Durmus and L. Toppare, *Adv, Mater.*, 2008, **20**, 691.
20 E. E. Havinga, W. Hoeve and H. Wynberg, *Synth. Met*., 1993, **55**, 299-306.
21 P. Nils-Krister, S. Mengtao, K. Par, P. Tonu and I. Olle, *J. Chem. Phys*., 2005, **123**, 204718-204726.
22 J. Pranata, R. H. Grubbs and D. A. Dougherty, *J. Am. Chem. Soc.*, 1988, **110**, 3430.
23 E. E. Havinga, W. Ten Hoeve and H. Wynberg, *Synth. Met*., 1993, **299**, 55-57.
24 A. Cihaner and F. Algı, *Adv. Funct, Mater.*, 2008, **18**, 3583.
25 G. Sonmez, C. K. F. Shen, Y. Rubin and F. Wudl, *Angew. Chem. Int. Ed.*, 2004, **43**, 1498.
26 G. Sonmez, H. B. Sonmez, C. K. F. Shen, R.W. Jost, Y. Rubin and F. Wudl, *Macromolecules*, 2005, **38**, 669.
27 E. Sefer and F. B. Koyuncu, *Electrochim Acta*, 2014, **143**, 106-113.
28 P. M. Beaujuge, S. Ellinger and J. R. Reynolds, *Nat. Mater.*, 2008, **7**, 795-799.
29 R. C. Coffin, J. Peet, J. Rogers and G. C. Bazan, *Nat. Chem.*, 2009, **1**, 657-661.
30 S. Hayashi and T. Koizumi, *Polym. Chem.*, 2012, **3**, 613-616.
31 D. M. Leeuw, M. M. Simenon, A. R. Brown and R. E. F. Einerhand, *Synth. Met.*, 1997, **87**, 53.
32 Z. Xu, J. H. Zhao, C. S. Cui, W. Y. Fan and J. f. Liu, *Electrochim Acta*, 2014, **125**, 241-249.
33 E. K. Unver, S. Tarkuc, Y. A. Udum, C. Tanyeli and L. Toppare, *Org. Electron*., 2011, **10**, 1625-1631.
34 Y. Tsubata, T. Suzuki, T. Miyashi and Y. Yamashita, *J. Org. Chem.*, 1992, **57**, 6749-6755.
35 Y. Zhang, W. Cui and Q. H. Cheng, *Sci. Technol. Chem. Indus.*, 2012, **20**, 38-41.
36 S. S. Zhu and T. M. Swager, *J. Am. Chem. Soc*., 1997, **119**, 12568-12577.
37 L. E. Harrington, J. F. Britten and M. J. McGlinchey, *Can. J. Chem.*, 2003, **81**, 1180-1186.
38 L. H. Xu, C. Su, C. Zhang and C. A. Ma, *Synth. Met*., 2011, **161**, 1856-1860.
39 S. Tarkuc, Y. A. Udum and L. Toppare, *Polymer*, 2009, **50**, 3458-3464.
40 G. Sonmez, H. Meng, Q. Zhang and F. Wudl, *Adv. Funct. Mater.*, 2003, **13**, 726.
41 H. W. Heuer, R. Wehrmann and S. Kirchmeyer, *Adv. Func. Mater.*, 2002, **12**, 89.
42 O. Bohnke, C. Bohnke and S. Amal, *Mater. Sci. Eng. B*, 1989, **197**, 1-2.
43 C. M. Amb, A. L. Dyer and J. R. Reynolds, *Chem. Mater.*, 2011, **23**, 397-415.
44 J. K. Xu, J. Hou, S. S. Zhang, Q. Xiao, R. Zhang, S. Z. Pu and Q. L. Wei, *J. Phys. Chem.* B, 2006, **110**, 2643-2648.
45 Y. Li, Y. Cao, J. Gao, D. Wang, G. Yu and A. Heeger, *Synth Met.*, 1999, **99**, 243.
46 J. Xu, H. Liu, S. Pu, F. Li and M. Luo, *Macromolecules*, 2006, **39**, 5611.
47 E. Sefer, H. Bilgili, B. Gultekin, M. Tonga and S. Koyuncu, *Dyes Pigments*, 2015, **113**, 121-128.
48 J. Hwang, J. I. Son and Y. -B. Shim, *Sol. Energy Mater. Sol. Cells*, 2010, **94**, 1286-1292.
49 H. Akpınar, A. Balan, D. Baran, E. K. Ünver and L. Toppare, *Polymer*, 2010, **51**, 6123-6131.
50 C. J. DuBois, K. A. Abboud and J. R. Reynolds, *J. Chem. Phys.*, 2004, **108**, 8550-8557.



 

51 B. Yigitsoy, S. Varis, C. Tanyeli, I. M. Akhmedov and L. Toppare, *Electrochim. Acta*, 2007, **52**, 6561-6568.
52 P. M. Beaujuge and J. R. Reynolds, *Chem. Rev.*, 2010, **110**, 268-320.
53 C. Bechinger, M. S. Burdis and J. G. Zhang, *Solid State Commun*., 1997, **101**, 753.

**Graphical Abstract**

# Effects of Alkyl or Alkoxy Side Chains on the Electrochromic Properties of Four Ambipolar Donor-Acceptor Type Polymers

Yanxia Liu, Min Wang, Jinsheng Zhao*, Chuansheng Cui and Jifeng Liu*

Four novel donor-acceptor type polymers exhibit superior p- and n-doping processes, lower optical band gaps, robust stabilities and excellent optical contrasts in NIR region. Two of them exhibit neutral green.